

# Exact universal excitation waveform for optimal enhancement of directed ratchet transport

Ricardo Chacón<sup>1</sup> and Pedro J. Martínez<sup>2</sup>

<sup>1</sup>Departamento de Física Aplicada, E. I. I., Universidad de Extremadura, Apartado Postal 382, E-06006 Badajoz, Spain and Instituto de Computación Científica Avanzada (ICCAEx), Universidad de Extremadura, E-06006 Badajoz, Spain. and

<sup>2</sup>Departamento de Física Aplicada, E.I.N.A., Universidad de Zaragoza, E-50018 Zaragoza, Spain and Instituto de Ciencia de Materiales de Aragón, CSIC-Universidad de Zaragoza, E-50009 Zaragoza, Spain.

(Dated: January 11, 2019)

The existence and properties of an *exact* universal excitation waveform for optimal enhancement of directed ratchet transport are deduced from the criticality scenario giving rise to ratchet universality, and confirmed by numerical experiments in the context of a driven overdamped Brownian particle subjected to a vibrating periodic potential. While the universality scenario holds regardless of the waveform of the periodic vibratory excitations involved, it is shown that the enhancement of directed ratchet transport is optimal when the impulse transmitted by those excitations (time integral over a half-period) is maximum. Additionally, the existence of a *frequency-dependent* optimal value of the relative amplitude of the two excitations involved is illustrated in the simple case of harmonic excitations.

PACS numbers:

The possibility of generating directed transport from a fluctuating environment without any net external force, the ratchet effect [1-3], has been a major research topic in distinct areas of science over the last few decades. The reasons are its potential applications for understanding such systems as molecular motors [4], protein translocation processes [5], and coupled Josephson junctions [6], and its wide range of potential technological applications including the design of micro- and nano-devices suitable for on-chip implementation. Directed ratchet transport (DRT) is now understood qualitatively to be a result of the interplay of nonlinearity, symmetry breaking [7], and non-equilibrium fluctuations including temporal noise [2], spatial disorder [8], and quenched temporal disorder [9]. But only recently have several fundamental aspects begun to be elucidated, including current reversals [10] and the quantitative dependence of DRT strength on the system's parameters [11]. At first sight, this aspect of controllability should be easier to investigate in non-chaotic physical contexts such as those of certain extremely small systems, including many nanoscale devices and systems occurring in biological and liquid environments, in which DRT is often suitably described by overdamped ratchets [2,12-14]. Thus, the interplay between thermal noise and symmetry breaking in the DRT of a Brownian particle moving on a periodic substrate subjected to a homogeneous temporal bicharmonic excitation has been explained quantitatively in coherence with the degree-of-symmetry-breaking (DSB) mechanism [15], as predicted by the theory of ratchet universality (RU) [16]. Since it has been demonstrated for temporal and spatial bicharmonic excitations that optimal enhancement of DRT is achieved when maximally effective (i.e., critical) symmetry breaking occurs, which implies the existence of a particular universal waveform whose *biharmonic* approximation is now known [16], the following fundamental

questions naturally arise: What is the *exact* waveform of such a universal periodic excitation? What are the geometric properties of the associated optimal ratchet potential?

We shall here deduce the existence and properties of such an exact universal excitation waveform from the criticality scenario, and explore its implications in the case of a driven Brownian particle moving in a back-and-forth travelling periodic potential [2] described by the overdamped model

$$\dot{x} + \sin[x - \gamma f(t)] = \sqrt{\sigma} \xi(t) + \gamma g(t), \quad (1)$$

where  $f(t), g(t)$  are temporal excitations with zero mean,  $f(t)$  is  $T$ -periodic,  $\gamma$  is an amplitude factor,  $\xi(t)$  is a Gaussian white noise with zero mean and  $\langle \xi(t) \xi(t+s) \rangle = \delta(s)$ , and  $\sigma = 2k_b T'$  with  $k_b$  and  $T'$  being the Boltzmann constant and temperature, respectively. Note that Eq. (1) is equivalent to

$$\begin{aligned} \dot{z} + \sin z &= \sqrt{\sigma} \xi(t) + \gamma F(t), \\ F(t) &\equiv g(t) - f(t), \end{aligned} \quad (2)$$

where  $z(t) \equiv x(t) - \gamma f(t)$ , and  $z$  and  $x$  are the particle phases relative to the vibrating potential frame and the laboratory frame, respectively. Since the mean velocity on averaging over different realizations of noise is the same in both frames,  $\langle \langle \dot{x} \rangle \rangle = \langle \langle \dot{z} \rangle \rangle$ , we shall consider Eq. (2) for convenience in our analysis. For the sake of clarity, we shall confine ourselves to the regime where the DRT mechanism dominates over the thermal inter-well activation mechanism [15]. Also, we shall show how RU allows the dependence of DRT velocity on the system's parameters to be explained quantitatively, and works effectively in two significant cases: (1) when  $F(t)$  is a truncated Fourier series of the exact universal periodic excitation after  $N \geq 2$  terms, and (2) when  $f(t)$  and

$g(t)$  are harmonic excitations. For deterministic ratchets, the effectiveness of the theory of RU has been demonstrated in diverse physical contexts in which the driving excitations are chosen to be biharmonic. Examples are cold atoms in optical lattices [17], topological solitons [9], Bose-Einstein condensates exposed to a sawtooth-like optical lattice potential [18], matter-wave solitons [11], and one-dimensional granular chains [19].

*Exact universal excitation waveform.*—Let us assume in this section that the excitation's amplitude and period are fixed. The criticality scenario giving rise to the existence of a universal excitation waveform which optimally enhances DRT is a consequence of two competing reshaping-induced effects: the increase in DSB and the decrease in the (normalized) maximal transmitted impulse over a half-period [16]. This means that the greater the impulse transmitted by a periodic excitation having its shift symmetry broken, the lower the DSB needed to yield the same strength of DRT, and vice versa. Since the strength of any transport, in the sense of the mean kinetic energy on averaging over different realizations of noise  $\langle\langle x^2 \rangle\rangle$ , depends upon the impulse transmitted by the driving excitation (see the Supplemental Material [20] for a detailed deduction), and the waveform yielding *maximal* transmitted impulse is that of a square-wave, the exact universal waveform should present a constant positive value,  $A$ , over a certain range  $t \in [0, \tau]$ ,  $0 < \tau < T$ , and a constant negative value,  $-B$ , over the remaining range  $t \in [\tau, T]$ , i.e., it should belong to the parameterized family of functions

$$\mathcal{F}(t) \equiv \frac{2(A+B)}{\pi} \sum_{n=1}^{\infty} \frac{\sin(n\pi\tau/T)}{n} \cos\left[\frac{2n\pi}{T}(t-\tau/2)\right]. \quad (3)$$

Clearly, the constraints  $A \neq B$  and  $\tau \neq T/2$  are *necessary* conditions to satisfy two requirements: the breaking of the shift symmetry and the zero-mean property of the exact universal excitation  $f_u(t)$ . This further requirement implies the relationship

$$\tau = T/(1 + A/B), \quad (4)$$

i.e., one only has to obtain the suitable value of either the asymmetry parameter  $\tau$  or  $A/B$  that makes the DSB maximally effective, thus providing the exact universal excitation waveform. The suitable value of  $A/B$  can be calculated from the quantifier of the DSB associated with the shift symmetry of  $f_u(t)$ ,  $D_s(f_u)$  [16]. To this end, we properly require that the (positive and negative) amplitudes of  $\mathcal{F}(t)$  and a suitable (symmetry-breaking-inducing) biharmonic excitation, for example  $f_{bh}(t) = \gamma [\eta \sin(\omega t) + (1-\eta) \sin(2\omega t + \varphi)]$  with  $\gamma > 0, \eta \in [0, 1], \varphi = \varphi_{opt} \equiv \pi/2$  [16], should be the same, i.e.,  $A = \max_t f_{bh}(t), B = -\min_t f_{bh}(t)$ . One thus ob-

tains straightforwardly

$$D_s(f_u) \equiv \frac{1}{T} \int_0^{T/2} \frac{-f_u(t+T/2)}{f_u(t)} dt = \frac{A}{B} = \begin{cases} 1 - \eta + \frac{\eta^2}{8(1-\eta)}, & \eta \leq \frac{4}{5} \\ 2\eta - 1, & \eta \geq \frac{4}{5} \end{cases}, \quad (5)$$

where an increase in the deviation of  $D_s(f_u)$  from 1 (unbroken symmetry) indicates an increase in the DSB. One finds that  $D_s(f_u)$  has the value  $D_s(f_u) |_{\eta=0,1} = 1$ , and presents, as a function of  $\eta$ , a single extremum at  $\eta = 2/3$  (see Fig. 1, top panel), and hence the DSB is maximum when  $A/B = 1/2, \tau = 2T/3$  [cf. Eqs. (4)-(5)].

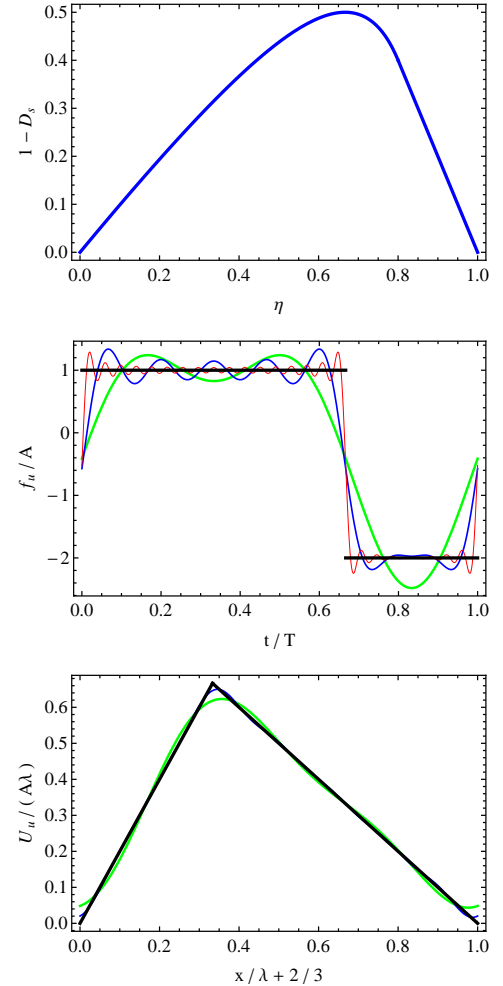


FIG. 1: Top: Quantifier of the DSB associated with the shift symmetry  $D_s$  vs amplitude factor  $\eta$  [cf. Eq. (5) and the text] for the exact universal excitation  $f_u(t)$  [cf. Eq. (6)]. Middle: Function  $f_u(t)$  and the truncations of its Fourier series after  $N = 2, 7, 25$  terms vs  $t$  (solid curves of respectively decreasing thickness). Bottom: Exact universal potential  $U_u(x)$  [cf. Eq. (7)] and the truncations of its Fourier series after  $N = 2, 7, 25$  terms vs  $x$  (solid curves of respectively decreasing thickness). The values of the steep and shallow slopes are 2 and -1, respectively.

As expected from a symmetry analysis, we obtained the same behaviour when using any other alternative form for  $f_{bh}(t)$  together with the corresponding suitable values of  $\varphi_{opt}$  in each case [16]. Therefore, the values  $A/B = 1/2, \tau = 2T/3$  fix the exact universal waveform of the excitation  $f_u(t)$  as well as the properties of the associated ratchet potential  $U_u(x) \equiv -\int f_u(x)dx$  (see Fig. 1, middle and bottom panels). In this regard, it is worth mentioning that the biparametric  $(A, B)$  family of dichotomous driving waveforms predicted in Ref. [21] for optimal enhancement of DRT in overdamped, adiabatic rocking ratchets includes (without indicating that it is a special case) the exact universal waveform of  $f_u(t)$  for the particular choice  $A/B = 1/2$ . After calculating the Fourier series of the universal excitation and potential,

$$f_u(t) \equiv \frac{6A}{\pi} \sum_{n=1}^{\infty} \frac{\sin(2n\pi/3)}{n} \cos[2n\pi(t/T - 1/3)], \quad (6)$$

$$U_u(x) \equiv -\frac{3A\lambda}{\pi^2} \sum_{n=1}^{\infty} \frac{\sin(2n\pi/3)}{n^2} \sin[2n\pi(x/\lambda - 1/3)], \quad (7)$$

where  $\lambda$  is the spatial period, one obtains the geometric properties of the universal ratchet potential per unit of amplitude and unit of spatial period [Eq. (7); see Fig. 1, bottom panel]. Next, we consider the case  $g(t) = 0$  and  $f(t) = -(1/A) \int f_{u,N}(t)dt$  [cf. Eq. (7)], i.e.,  $F(t) \equiv f_{u,N}(t)/A$  in Eq. (2), with  $f_{u,N}(t)$  being the Fourier series of  $f_u(t)$  truncated after  $N$  terms [cf. Eq. (6)]. Our numerical results systematically indicate an overall increase of the maximum value of  $\langle\langle\dot{z}\rangle\rangle$  with the number of terms  $N$ , while keeping the remaining parameters constant. Moreover, the typical instance shown in Fig. 2 (top panel) indicates that the average velocity (absolute value) quickly increases with  $N$ , and reaches its asymptotic value for  $N \sim 13$ . This behaviour is found to be correlated with that of the impulse per unit of amplitude transmitted by  $f_{u,N}(t)$  over a half-period,

$$I_N \equiv \frac{1}{T} \int_0^{T/2} f_{u,N}(t) dt = \frac{3}{\pi^2} \sum_{i=1}^N \frac{\sin(\frac{2i\pi}{3}) [\sin(\frac{i\pi}{3}) + \sin(\frac{2i\pi}{3})]}{i^2}, \quad (8)$$

as expected from the theory of RU [16] (see Fig. 2, bottom panel).

*Harmonic excitations.*—For the sake of completeness, we next explore the standard case [2] in which the two temporal excitations involved are harmonic:  $f(t) \equiv \eta \cos(\omega t)$ ,  $g(t) \equiv (1 - \eta) \cos(2\omega t + \varphi)$ ,  $\omega \equiv 2\pi/T$ ,  $\eta \in [0, 1]$  in Eq. (1), i.e.,

$$F(t) \equiv \eta \omega \sin(\omega t) + (1 - \eta) \cos(2\omega t + \varphi) \quad (9)$$

in Eq. (2). Leaving aside the effect of noise (an effective change of the potential barrier which is in turn controlled by the DSB mechanism [15]), RU predicts (for  $\sigma = 0$ )

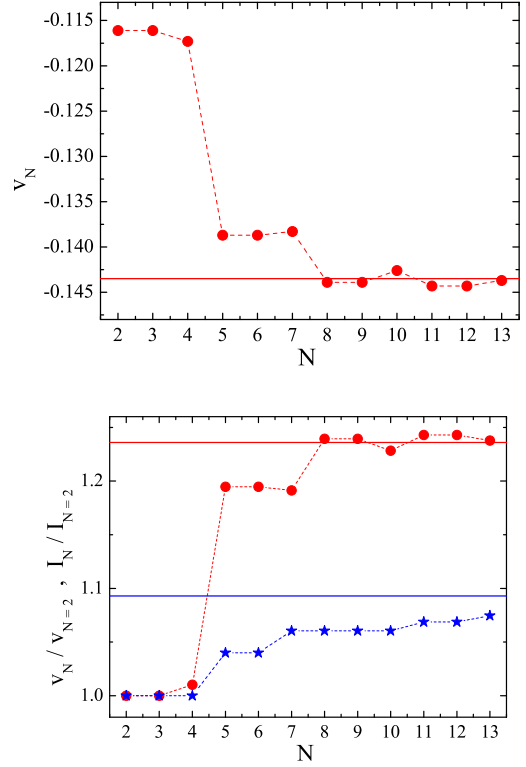


FIG. 2: Top: Average velocity  $v_N \equiv \langle\langle\dot{z}\rangle\rangle$  [cf. Eq. (2); dots] as a function of the number,  $N$ , of harmonics which are retained in the truncated Fourier series of  $f_u(t)$  [cf. Eq. (6)]. The horizontal line indicates the asymptotic value of the average velocity corresponding to the complete series of  $f_u(t)$ . Bottom: Normalized average velocity (dots) and normalized impulse [cf. Eq. (8); stars] as functions of the number of harmonics,  $N$ . The horizontal lines indicate the respective asymptotic values when  $N \rightarrow \infty$ . The dashed lines connecting the symbols are solely to guide the eye. Fixed parameters:  $\gamma = 8, T = 4\pi, \sigma = 0.8$ .

that the optimal value of the relative amplitude  $\eta$  comes from the condition that the amplitude of  $\sin(\omega t)$  must be twice as large as that of  $\cos(2\omega t + \varphi)$  in Eq. (2) with  $F(t)$  given by Eq. (9), and the optimal values of the initial phase difference are  $\varphi = \varphi_{opt} \equiv \{0, \pi\}$  [16]. Thus, RU predicts the existence of a *frequency-dependent* optimal value of  $\eta$ :

$$\eta_{opt} \equiv 2/(2 + \omega), \quad (10)$$

and, equivalently, an optimal frequency for each value of  $\eta$ :  $\omega_{opt} \equiv 2(1 - \eta)/\eta$ . Numerical simulations confirmed this prediction over a wide range of frequencies (see Fig. 3, top panel). As mentioned above, the numerical estimate of the  $\eta$  value at which the average velocity presents an extremum,  $\eta_{opt}^{\sigma>0}$ , is slightly lower than the corresponding value  $\eta_{opt}$  [Eq. (10)], as expected [15] (see Fig. 3, bottom panel). It is worth noting that the property Eq. (10) represents a genuine feature of the back-

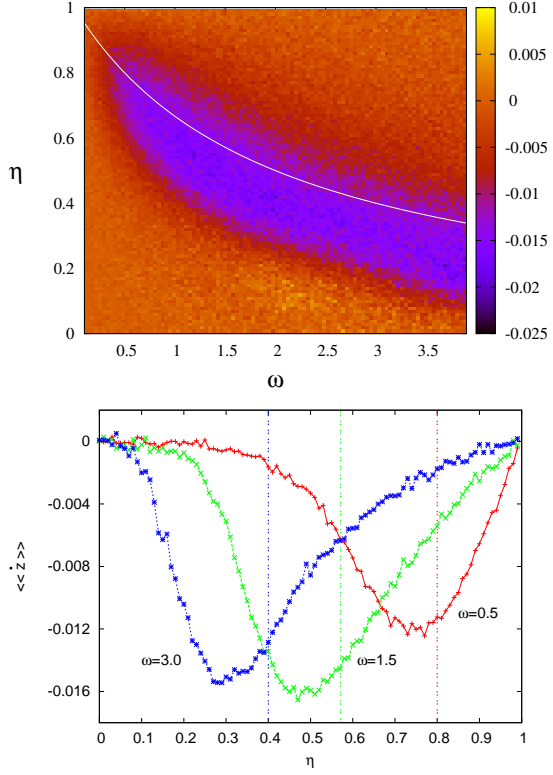


FIG. 3: Top: Average velocity  $\langle\langle\dot{z}\rangle\rangle$  [cf. Eq. (2)] vs relative amplitude  $\eta$  and frequency  $\omega$  for  $F(t) \equiv \eta\omega \sin(\omega t) + (1 - \eta)\cos(2\omega t + \varphi)$  [cf. Eq. (9)]. Also plotted is the theoretical prediction for the maximum average velocity [cf. Eq. (10); solid curve]. Bottom:  $\langle\langle\dot{z}\rangle\rangle$  vs  $\eta$  for three values of the frequency:  $\omega = 0.5, 1.5, 3$ . The vertical dashed lines indicate the respective predicted optimal values of  $\eta$  for  $\sigma = 0$  [cf. Eq. (10)]. Fixed parameters:  $\varphi = \varphi_{opt} = 0, \sigma = 10, \gamma = 15$ .

and-forth travelling potential ratchet [Eq. (1)] which is absent in the case of an overdamped rocking ratchet [15]. Also, this finding is in sharp contrast with the prediction coming from *all* the earlier theoretical approaches [3,7, 22-24], namely, that the dependence of the average velocity should scale as

$$\langle\langle\dot{z}\rangle\rangle \sim \gamma^3 \omega^2 \eta^2 (1 - \eta), \quad (11)$$

which fails to explain the observed phenomenology (cf. Fig. 3). It is worth mentioning that the case where the roles played by the harmonic excitations  $\eta \cos(\omega t)$  and  $(1 - \eta)\cos(2\omega t + \varphi)$  are interchanged presents different optimal values of the initial phase  $\varphi$  and a different dependence on the frequency of the optimal value of  $\eta$ , and that numerical simulations again confirmed these predictions from RU (see the Supplemental Material [20] for analytical and numerical details). To confirm the aforementioned characteristics of the criticality scenario giving rise to the existence of the exact universal excitation waveform, we compared the ratchet effectiveness of the biharmonic excitation [Eq. (9)] with that of  $F(t) \equiv \mathcal{F}(t)$  [cf. Eq. (3)] subjected to the requirement

that both excitations have the same (positive and negative) amplitudes for each value of  $\eta$ . Recall that varying the amplitudes of  $\mathcal{F}(t)$  implies varying the asymmetry parameter  $\tau$ , and vice versa [cf. Eq. (4)], whence both  $\tau$  and  $A/B$  will be  $\eta$ -dependent so as to allow a proper comparison of the ratchet effectiveness of these excitations. Indeed, the results shown in Fig. 4 indicate that the DRT strength of the dichotomous excitation is greater than that of the biharmonic excitation over (almost) the *entire* range of  $\eta$  values, i.e., enhancement of DRT occurs when the impulse transmitted is maximum regardless of the DSB of the two excitations. One clearly sees in Fig. 4 that the greater the impulse transmitted, the lower the DSB needed to yield the same strength of DRT, and vice versa, as predicted from the criticality scenario. Note that the noise-induced decrease of the optimal value of  $\eta$  with respect to the corresponding deterministic prediction,  $\eta_{opt}^{\sigma=0} - \eta_{opt}^{>0}$  [ $\eta_{opt}^{\sigma=0} = 0.8$ ; cf. Eq. (10)], is slightly lower when the transmitted impulse is maximum. This provides additional evidence for the impulse being the main quantifier of the driving effectiveness of a periodic excitation.

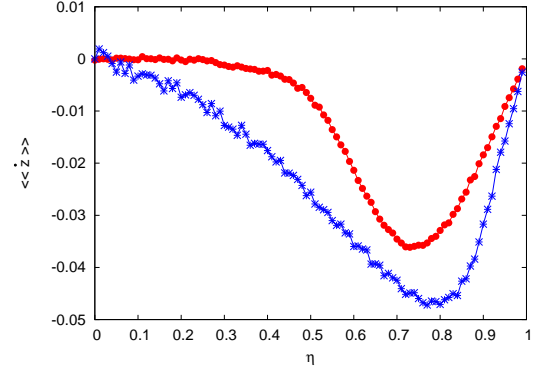


FIG. 4: Average velocity  $\langle\langle\dot{z}\rangle\rangle$  [cf. Eq. (2)] vs parameter  $\eta$  (see the text) for two choices of the excitation  $F(t)$ :  $\eta\omega \sin(\omega t) + (1 - \eta)\cos(2\omega t + \varphi)$  [cf. Eq. (9); dots] and  $\mathcal{F}(t)$  [cf. Eq. (3); stars]. The lines connecting the symbols are solely plotted to guide the eye. Fixed parameters:  $\gamma = 8, T = 4\pi, \varphi = \varphi_{opt} = 0, \sigma = 4$ .

Additionally, robustness of the present universality scenario is also observed when the external periodic excitation is replaced by a chaotic excitation having the same underlying main frequency in its Fourier spectrum (see the Supplemental Material [20]).

*Conclusions.*—In summary, from the criticality scenario giving rise to ratchet universality we have demonstrated the existence and properties of an exact universal excitation waveform for optimal enhancement of directed ratchet transport. Our numerical experiments confirmed those findings, as well as revealed other unanticipated properties for the standard case of harmonic excitations in the general context of a driven overdamped Brownian particle subjected to a vibrating periodic potential. The exact universal waveform is the *simplest* possible (a par-

ticular dichotomous waveform), and is far more efficient than its biharmonic approximation, and the waveform of the associated optimal ratchet potential is therefore a particular case of the simplest piecewise waveform as is used, for instance, in a flashing ratchet. Since most models of biological Brownian motors are compatible with a simplified description based on the flashing ratchet, we are tempted to conjecture that the universal optimal ratchet potential could underlie the complex biological machinery operating at the nanoscale as a result of a

process of Darwinian optimization.

R.C. acknowledges financial support from the Junta de Extremadura (JEx, Spain) through Project No. GR18081 cofinanced by FEDER funds. P.J.M. acknowledges financial support from the Ministerio de Economía y Competitividad (MINECO, Spain) through project FIS2017-87519 cofinanced by FEDER funds and from the Gobierno de Aragón (DGA, Spain) through grant E36\_17R to the FENOL group.

---

[1] R. P. Feynman, R. B. Leighton, and M. Sands, *The Feynman Lectures on Physics* (Addison Wesley, Reading, 1966) Vol. 1, Chapt. 46.

[2] P. Reimann, Phys. Rep. **361**, 57 (2002).

[3] P. Hänggi and F. Marchesoni, Rev. Mod. Phys. **81**, 387 (2009).

[4] F. Jülicher, A. Ajdari, and J. Prost, Rev. Mod. Phys. **69**, 1269 (1997).

[5] M. Gu and C. M. Rice, Proc. Natl. Acad. Sci. U.S.A. **107**, 521 (2010).

[6] Jing-hui Li, Phys. Rev. E **67**, 061110 (2003).

[7] S. Flach, O. Yevtushenko, and Y. Zolotaryuk, Phys. Rev. Lett. **84**, 2358 (2000); S. Denisov, S. Flach, A. A. Ovchinnikov, O. Yevtushenko, and Y. Zolotaryuk, Phys. Rev. E **66**, 041104 (2002).

[8] A. B. Kolton, Phys. Rev. B **75**, 020201(R) (2007).

[9] P. J. Martínez and R. Chacón, Phys. Rev. Lett. **100**, 144101 (2008).

[10] J. L. Mateos, Phys. Rev. Lett. **84**, 258 (2000); P. Malgarotti, I. Pagonabarraga, and D. Frenkel, Phys. Rev. Lett. **109**, 168104 (2011); A. Wickenbrock, D. Cubero, N. A. Abdul Wahab, P. Phoonthong, and F. Renzoni, Phys. Rev. E **84**, 021127 (2011).

[11] M. Rietmann, R. Carretero-González, and R. Chacón, Phys. Rev. A **83**, 053617 (2011).

[12] G. Carapella and G. Costabile, Phys. Rev. Lett. **87**, 077002 (2001).

[13] F. R. Alastrite and J. L. Mateos, Physica A **372**, 263 (2006).

[14] R. Gommers, S. Bergamini, and F. Renzoni, Phys. Rev. Lett. **95**, 073003 (2005).

[15] P. J. Martínez and R. Chacón, Phys. Rev. E **87**, 062114 (2013); **88**, 019902(E) (2013); **88**, 066102 (2013).

[16] R. Chacón, J. Phys. A: Math. Theor. **40**, F413 (2007); **43**, 322001 (2010).

[17] M. Schiavoni, L. Sánchez-Palencia, F. Renzoni, and G. Grynberg, Phys. Rev. Lett. **90**, 094101 (2003); R. Chacón, arXiv:1802.02826 (2018).

[18] T. Salger *et al.*, Science **326**, 1241 (2009).

[19] V. Berardi, J. Lydon, P. G. Kevrekidis, C. Daraio, and R. Carretero-González, Phys. Rev. E **88**, 052202 (2013).

[20] See Supplemental Material at <http://xxx> for details on (A) the energy analysis, (B) the case where the roles of the harmonic excitations are interchanged, and (C) the case where the external periodic excitation is substituted by a chaotic excitation.

[21] S. J. Lade, J. Phys. A: Math. Theor. **41**, 275103 (2008).

[22] F. Marchesoni, Phys. Lett. A **119**, 221 (1986).

[23] N. R. Quintero, J. A. Cuesta, and R. Alvarez-Nodarse, Phys. Rev. E **81**, 030102(R) (2010).

[24] S. Denisov, S. Flach, and P. Hänggi, Phys. Rep. **538**, 77 (2014).

## I. SUPPLEMENTARY MATERIAL

### A. Energy-based analysis

In this section we deduce an analytical expression for the mean kinetic energy on averaging over different realizations of noise of a Brownian particle of mass  $m$  which satisfies the general equation of motion

$$m\ddot{x} + \frac{dU}{dx} = -\mu\dot{x} + \gamma f(t) + \sqrt{\sigma}\xi(t), \quad (\text{S1})$$

where  $U(x)$  is a potential subject to a lower bound (i.e.,  $\exists \alpha \in \mathbb{R} / U(x) \geq \alpha \forall x$ ),  $f(t)$  is a unit-amplitude  $T$ -periodic function with zero mean,  $\xi(t)$  is a Gaussian white noise of zero mean and  $\langle \xi(t)\xi(t+s) \rangle = \delta(s)$ , and  $\sigma = 2\mu k_b T'$  with  $k_b$  and  $T'$  being the Boltzmann constant and temperature, respectively. Also, we assume without loss of generality that  $f(0 \leq t \leq T^*) \geq 0$  and define the impulse transmitted by  $f(t)$  (per unit of amplitude) as

$$I \equiv \int_{nT}^{nT+T^*} f(t) dt > 0, \quad n = 0, 1, 2, \dots. \quad (\text{S2})$$

Equation S1 has the associated energy equation

$$\frac{dE}{dt} = -\mu\dot{x}^2 + \gamma\dot{x}f(t) + \sqrt{\sigma}\dot{x}\xi(t), \quad (\text{S3})$$

where  $E(t) \equiv (m/2)\dot{x}^2(t) + U[x(t)]$  is the energy function. Integration of Eq. S3 over the intervals  $[nT, nT + T^*]$  and  $[nT + T^*, (n+1)T]$ ,  $n = 0, 1, 2, \dots$ , yields

$$E(nT + T^*) = E(nT) - \mu \int_{nT}^{nT+T^*} \dot{x}^2(t) dt + \sqrt{\sigma} \int_{nT}^{nT+T^*} \dot{x}(t)\xi(t) dt + \gamma \int_{nT}^{nT+T^*} \dot{x}(t)f(t) dt, \quad (\text{S4})$$

$$E[(n+1)T] = E(nT + T^*) - \mu \int_{nT+T^*}^{(n+1)T} \dot{x}^2(t) dt + \sqrt{\sigma} \int_{nT+T^*}^{(n+1)T} \dot{x}(t)\xi(t) dt + \gamma \int_{nT+T^*}^{(n+1)T} \dot{x}(t)f(t) dt, \quad (\text{S5})$$

respectively, where the second integrals in Eqs. S4 and S5 are considered in the Stratonovich sense. After applying the first mean value theorem for integrals [1] to the last integrals on the right-hand sides of Eqs. S4 and S5, using Eq. S2, and recalling that  $f(t)$  is a zero-mean function, one obtains

$$E(nT + T^*) = E(nT) - \mu \int_{nT}^{nT+T^*} \dot{x}^2(t) dt + \sqrt{\sigma} \int_{nT}^{nT+T^*} \dot{x}(t)\xi(t) dt + \gamma\dot{x}_n I, \quad (\text{S6})$$

$$E[(n+1)T] = E(nT + T^*) - \mu \int_{nT+T^*}^{(n+1)T} \dot{x}^2(t) dt + \sqrt{\sigma} \int_{nT+T^*}^{(n+1)T} \dot{x}(t)\xi(t) dt - \gamma\dot{x}'_n I, \quad (\text{S7})$$

respectively, where the discrete variables  $\dot{x}_n \equiv \dot{x}(t_n)$ ,  $\dot{x}'_n \equiv \dot{x}(t'_n)$ , with  $t_n$  and  $t'_n$  being unknown instants which only have to satisfy the respective relationships  $nT \leq t_n \leq nT + T^*$  and  $nT + T^* \leq t'_n \leq (n+1)T$ , according to the first mean value theorem for integrals. After adding Eqs. S6 and S7 from  $n = 0$  to  $n = N - 1$  and dividing the result by  $NT$ , one obtains

$$\frac{E(NT) - E(0)}{NT} = -\frac{\mu}{NT} \int_0^{NT} \dot{x}^2(t) dt + \gamma I \sum_{n=0}^{N-1} \left[ \frac{\dot{x}_n - \dot{x}'_n}{NT} \right] + \frac{\sqrt{\sigma}}{NT} \int_0^{NT} \dot{x}(t)\xi(t) dt. \quad (\text{S8})$$

Upon taking the limit  $N \rightarrow \infty$  in Eq. S8, averaging over different realizations of noise, and recalling that the system S1 is dissipative and that  $\xi(t)$  is a stationary random process which cannot contain a shot noise component, one finally obtains

$$\langle \langle \dot{x}^2 \rangle \rangle = \frac{\gamma I}{\mu} \left[ \langle \langle \dot{x}_n \rangle \rangle - \langle \langle \dot{x}'_n \rangle \rangle \right] + \frac{\sqrt{\sigma}}{\mu} \langle \langle \dot{x}\xi \rangle \rangle. \quad (\text{S9})$$

The following remarks are now in order. First,  $\langle\langle\dot{x}_n\rangle\rangle$  provides the average of the particle's velocity when  $\dot{x}$  is measured exclusively at certain instants for which  $f(t)$  has the same sign as the acceleration  $\ddot{x}$  (cf. Eq. S1), i.e., when  $f(t)$  tends to yield an increase in the particle's velocity, while  $\langle\langle\dot{x}'_n\rangle\rangle$  does the same when  $f(t)$  has the opposite sign to  $\ddot{x}$ , i.e., when  $f(t)$  tends to yield a decrease in the particle's velocity. One sees from Eq. S9 that the effect of the difference  $\langle\langle\dot{x}_n\rangle\rangle - \langle\langle\dot{x}'_n\rangle\rangle$  on the average kinetic energy is modulated by the impulse per unit of amplitude, while keeping the remaining parameters constant. Second, increasing the noise strength from  $\sigma = 0$  activates the term  $\langle\langle\dot{x}\xi\rangle\rangle$ , which can be positive or negative.

### B. Complementary case of harmonic excitations

Let us consider the case of harmonic excitations in the main text's Eq. (1) when the roles of the excitations  $\eta \cos(\omega t)$  and  $(1 - \eta) \cos(2\omega t + \varphi)$  are interchanged, i.e., the Langevin equation now reads

$$\dot{x} + \sin[x - \gamma(1 - \eta) \cos(2\omega t + \varphi)] = \sqrt{\sigma}\xi(t) + \gamma\eta \cos(\omega t). \quad (\text{S10})$$

In the reference frame associated with the vibrating potential, one then obtains

$$\dot{z} + \sin z = \sqrt{\sigma}\xi(t) + \gamma[\eta \cos(\omega t) + 2\omega(1 - \eta) \sin(2\omega t + \varphi)], \quad (\text{S11})$$

where  $z(t) \equiv x(t) - \gamma(1 - \eta) \cos(2\omega t + \varphi)$ . Once again, ratchet universality predicts that the optimal value of the relative amplitude  $\eta$  comes from the condition that the amplitude of  $\cos(\omega t)$  must be twice as large as that of  $\sin(2\omega t + \varphi)$  in Eq. S11, while the optimal values of the initial phase difference are  $\varphi = \varphi_{opt} \equiv \{\pi/2, 3\pi/2\}$  [2]. It therefore predicts the existence of a *different* (with respect to the case considered in the main text, cf. Eq. (10)) frequency-dependent optimal value of  $\eta$ :

$$\eta_{opt} \equiv \frac{4\omega}{1 + 4\omega}, \quad (\text{S12})$$

and, equivalently, a different optimal frequency for each value of  $\eta$ :

$$\omega_{opt} \equiv \frac{\eta}{4(1 - \eta)}. \quad (\text{S13})$$

Numerical simulations (as shown in Fig. S1) confirmed this new prediction over a wide range of frequencies.

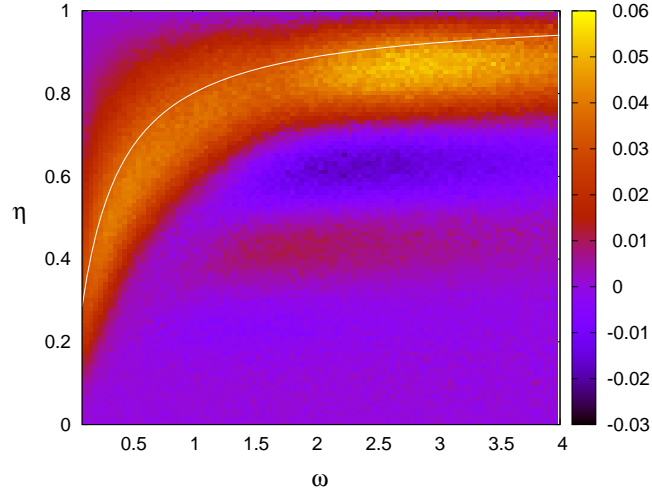


FIG. S1: Average velocity  $\langle\langle\dot{z}\rangle\rangle$  (cf. Eq. S11) vs relative amplitude  $\eta$  and frequency  $\omega$  for the parameters  $\varphi = \varphi_{opt} = \pi/2, \sigma = 4, \gamma = 8$ . Also plotted (solid line) is the theoretical prediction for the maximum average velocity (cf. Eq. S12).

### C. Robustness against chaotic excitations

In this section, we study the robustness of the universality scenario against the presence of a bounded chaotic excitation instead of an external periodic excitation. We shall consider the simple case  $f(t) \equiv \eta \cos(\omega t + \varphi/2)$ ,  $g(t) \equiv (1 - \eta) \alpha \dot{y}(t)$ ,  $\omega \equiv 2\pi/T$ ,  $\eta \in [0, 1]$  in the main text's Eq. (1), i.e.,

$$F_{\text{chaos}}(t) \equiv \eta \omega \sin(\omega t + \varphi/2) + (1 - \eta) \alpha \dot{y}(t) \quad (\text{S14})$$

in the main text's Eq. (2), where  $\dot{y}(t)$  is a chaotic response of a master system exhibiting the same underlying main frequency,  $2\omega$ , in its Fourier spectrum [cf. main text's Eq. (9)], but cannot itself yield directed ratchet transport (DRT). The value of  $\alpha$  is chosen in order for the excitations  $\cos(2\omega t + \varphi)$  and  $\alpha \dot{y}(t)$  to have similar ranges. We considered the following master system (damped driven pendulum)

$$\ddot{y} + K \sin y = -\delta \dot{y} + F \cos(2\omega_0 t), \quad (\text{S15})$$

with the parameter values  $\omega_0 = 0.5$ ,  $K = 2.25$ ,  $\delta = 0.375$ ,  $F = 2.48625$ , for which the pendulum presents a chaotic attractor irrespective of the initial conditions. Figure S2(a) shows the time series corresponding to the velocity  $\dot{y}(t)$ , and Fig. S2(b) shows the corresponding power spectrum which presents its main peak at the frequency  $2\omega_0$ . Note the presence of additional peaks at the frequencies  $6\omega_0, 10\omega_0, 14\omega_0, \dots$ , i.e., the underlying periodic solution,  $f(t)$ , only presents odd harmonics and hence satisfies the shift symmetry  $f(t + T/2) = -f(t)$  with  $T = \pi/\omega_0$ . This means that the function  $f(t)$  itself cannot yield directed ratchet transport.

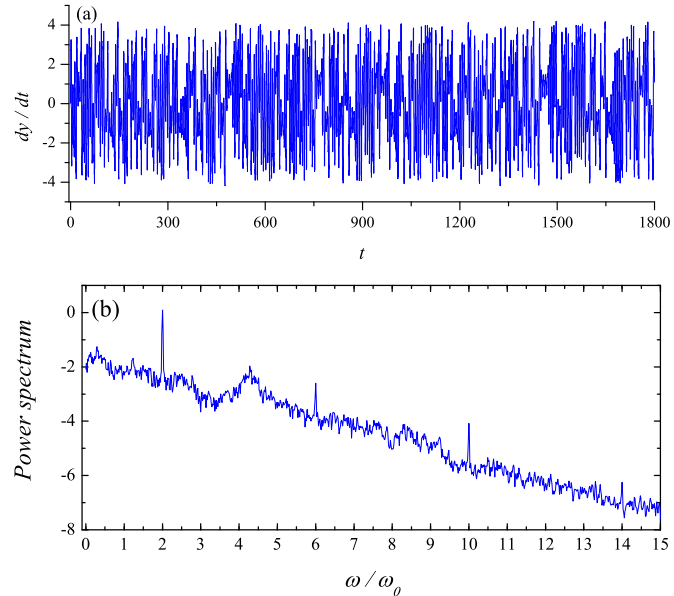


FIG. S2: (a) Velocity time series of  $\dot{y}(t)$ , and (b) the corresponding power spectrum ( $\log_{10} |S(\omega)|$  versus  $\omega/\omega_0$ ) associated with the damped driven pendulum given by Eq. S14. Fixed parameters:  $\omega_0 = 0.5$ ,  $K = 2.25$ ,  $\delta = 0.375$ ,  $F = 2.48625$ .

We found numerically the same dependence of the average velocity on  $\eta$  as in the deterministic case [main text's Eq. (9)], but with a drastic decrease of the DRT strength (see Fig. S3, top panel). Indeed, the presence of other noticeable harmonics in the Fourier spectrum of  $\dot{y}(t)$  [cf. Fig. S2(b)] yields interferences with the excitation  $\eta \omega \sin(\omega t)$  which leads  $F_{\text{chaos}}(t)$  to deviate from the optimal biharmonic approximation [cf. main text's Eq. (9)]. This phenomenon and the inherent noise background lead to  $F_{\text{chaos}}(t)$  losing DRT effectiveness, but without deactivating the DSB mechanism, and also to an additional decrease in the optimal value of  $\eta$  with respect to the corresponding deterministic prediction [cf. main text's Eq. (10)]. This robustness is also manifest in the dependence of the average velocity on  $\varphi$  (see Fig. S3, bottom panel).

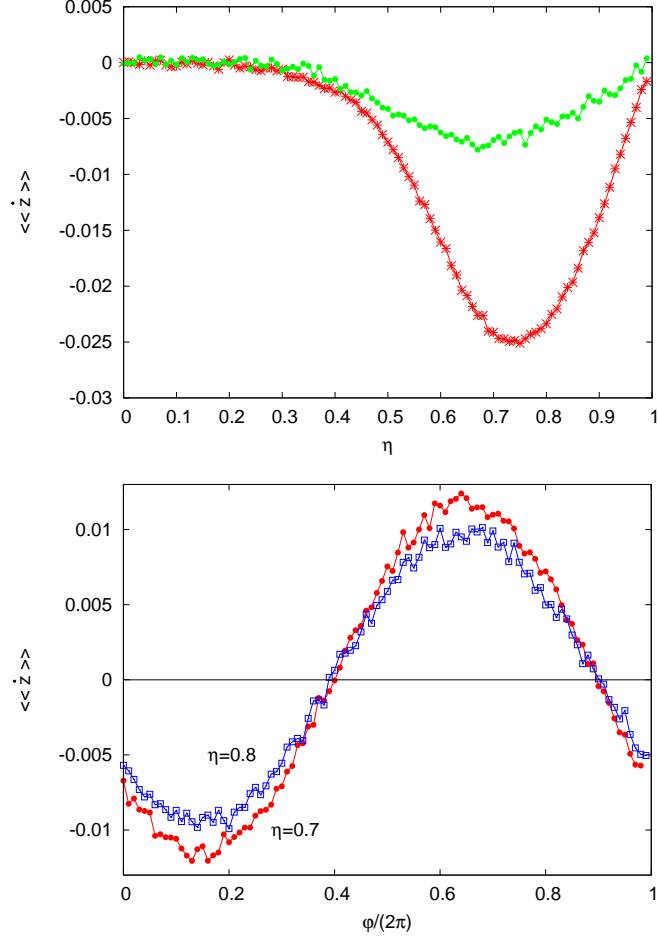


FIG. S3: Top: Average velocity  $\langle\langle z \rangle\rangle$  [cf. main text's Eq. (2)] vs parameter  $\eta$  for  $f(t) = \eta \cos(\omega t + \varphi/2)$ ,  $\varphi = \varphi_{opt} = 0$ , and two excitations  $g(t)$  having the same underlying main frequency,  $2\omega$ , in their Fourier spectrum: chaotic excitation [cf. Eqs. S14 and S15; dots] and deterministic excitation [cf. main text's Eq. (9); stars]. Bottom:  $\langle\langle z \rangle\rangle$  vs  $\varphi$  for the chaotic excitation and  $\eta = \{0.7, 0.8\}$ . The lines connecting the symbols are solely to guide the eye. Fixed parameters:  $\gamma = 8, T = 4\pi, \sigma = 5, \alpha = 0.25$ .